electronics

MDPI

Article

An Alternative Carrier-Based Implementation of Space Vector Modulation to Eliminate Common Mode Voltage in a Multilevel Matrix Converter

Janina Rząsa

Department of Power Electronics and Power Engineering, Rzeszow University of Technology, 35-959 Rzeszow, Poland; jrzasa@prz.edu.pl; Tel.: +48-017-865-1976

Received: 13 December 2018; Accepted: 30 January 2019; Published: 6 February 2019

Abstract: The main aim of the paper is to find a control method for a multilevel matrix converter (MMC) that enables the elimination of common mode voltage (CMV). The method discussed in the paper is based on a selection of converter configurations and the instantaneous output voltages of MMC represented by rotating space vectors. The choice of appropriate configurations is realized by the use of space vector modulation (SVM), with the application of Venturini modulation functions. A multilevel matrix converter, which utilizes a multilevel structure in a traditional matrix converter (MC), can achieve an improved output voltage waveform quality, compared with the output voltage of MC. The carrier-based implementation of SVM is presented in this paper. The carrier-based implementation of SVM avoids any trigonometric and division operations, which could be required in a general space vector approach to the SVM method. With use of the proposed control method, a part of the high-frequency output voltage distortion components is eliminated. The application of the presented modulation method eliminates the CMV in MMC what is presented in the paper. Additionally, the possibility to control the phase shift between the appropriate input and output phase voltages is obtained by the presented control strategy. The results of the simulation and experiment confirm the utility of the proposed modulation method.

Keywords: multilevel matrix converter; rotating voltage space vector; common move voltage; space vector pulse width modulation; venturini control method

1. Introduction

A multilevel matrix converter (MMC) is a frequency converter, whose topology [1–8] was proposed by analogy to multilevel inverters and its aim is the reduction of the voltage rating of the switches with respect to the supply voltages and the further improvement of the synthesized current and voltage waveforms. Two scientific centres paid attention to the analysis of MMC operations and two different control methods were developed there. The authors of papers [5–8] concentrate on the use of the space vector modulation (SVM) method, whereas in papers [2–4], the implementation of the Venturini control method is presented. The main goal in using either of the modulation methods in controlling MMC is the synthesis of the referenced sinusoidal output voltage and sinusoidal input current by controlling the input displacement angle. The application of these methods is involved with appearing CMV on the output terminals. The problem with appearing CMV is concerned with all the converters being controlled by the use of the pulse width modulation (PWM) method, both indirect frequency converters with a DC link, as well as a direct matrix converter (MC) and MMC. Because the topology of MMC is the modification of conventional MC, the analysis of the cancelation methods of CMV used in MC would be valuable in finding the control method to eliminate the CMV in MMC.

As for MC, many different methods have been reported to mitigate the detrimental influences of the CMV. The majority of the methods are based on a modification of SVM by the elimination of

the zero-space vector, as a complement of the switching cycle and replacement of the zero vectors by rotating space vectors or by active vectors, with minimum absolute values [9–12]. The authors of References [9,10] found that, in MC controlled by the use of SVM using rotating vectors, instead of zero vectors, had 42% lower CMV. The voltage transfer ratio (VTR) was found to be higher than 0.5. Next, in Reference [12], the controlling method of CMV reduction is achieved by using the switch configurations that connect each input phase to a different output phase, which means that rotating space vectors are used or the configurations connect all the output phases to the input phase, with the minimum absolute voltage. The authors found that the result of the CMV peak value reduction was 45.4%, while the VTR was 0.5% and 42.3%, when the VTR was higher. The next is the method that targeted the operation of the drive for a higher modulation index range ($0.577 \leq m \leq 0.866$) [12]. This method eliminates the zero vectors but continues to use active voltage vectors, with normalized duty ratios. The elimination of zero vectors reduces the peak value of CMV by 42%. Even though these methods, with their own modulation strategies, can produce a sound output performance within the specified operating range, they are applicable only to a limited VTR range. To achieve a sound output performance for the whole VTR range, these different modulation strategies should be properly combined. However, it is inconvenient to combine each method with the different switching patterns, because each modulation method, with its own formulae, uses different vectors to calculate the duty cycles. The main goal of the article is to present the control method that results in the elimination of CMV in MMC. The entire elimination of CMV in MC and in MMC is possible only by the use of such configurations, resulting from on-off states of bidirectional switches, which realize the rotating voltage space vectors.

In the application to MC, the use of the only rotating voltage space vectors to obtain the entire elimination of CMV is presented in References [13–19]. The author of Reference [13] compares the CMV in MC, controlled by the use of the Venturini method, which solely applies rotating space vectors, using the scalar control method and SVM control method, applying active and zero-space vectors. To obtain the cancelation of CMV in MC, the authors of Reference [14] introduce the new SVM and develop the modification of four-step commutation. The modification of the four-step commutation is dictated by the fact that, during the four-step commutation, such switch configurations arise, which are represented by active space vectors, what results in the high value of CMV. The SVM technique, solely using rotating space vectors, is also applied by the authors of References [15,19] in the modulation of dual MCs. Next, in Reference [20], the authors present a carrier-based implementation of SVM for dual MCs using only rotating space vectors. The advantage of the proposed strategy is an alternative way to achieve SVM, which does not involve the knowledge of space vectors, when it is derived. Additionally, it avoids any trigonometric and division operations that could be needed to implement the SVM using the general space vector approach.

In reference to MMC, an elimination of CMV is discussed in References [21,22] but the method presented there does not rely on the use solely of rotating space vectors in the synthesis of the output voltage. The authors of References [21,22] use space vector modulation, applying active and zero space voltage vectors. This method demands many trigonometric and division operations. The method analysed in References [21,22] results in only a 50% reduction in the peak value of CMV.

To solve the problem of the elimination of CMV in MMC, the author of the paper proposes the application of the modulation method, using solely rotating space vectors. To determine the switch duty cycles of MMC, the carrier-based implementation of SVM was used, which makes the application of the modulation method easy. The advantage of the proposed strategy is an alternative way to achieve SVM, which does not involve the knowledge of space vectors, when it is implemented. Additionally, it avoids any trigonometric and division operations that could be needed to implement the SVM, using the general space vector approach. The elaboration of the proposed method required the analysis of admissible switch configurations and the characteristics of their corresponding space vectors. The switch configurations and space vectors, providing the synthesis of the required output voltage and the elimination of CMV, were selected and presented in the paper.

In the MMC controlled by the implementation of the proposed method, the output voltage containing the fundamental component and high-frequency distortion components, with considerably less amplitudes, compared with the distortion component in the output voltage of MC, is synthesized. The next advantage of the method is that it obtains, in simulation tests, the entire cancelation of CMV and the reduction of the peak value of CMV to 12% of the peak value of the output voltage. This paper also presents the possibility to control the phase shift between the output voltage and appropriate input voltage. Controlling the phase shift between the output and input voltage may be important when working with the same output and input frequency of MMC and it could be applied as a converter in a Flexible AC Transmission System (FACTS) [23] to control the power flow or compensate the voltage dips.

The paper is organized in a total of five sections. The second section describes the topology of MMC, the admissible configuration of the analysed converter and the output voltage space vectors. The proposed modulation method is described in the third section. The fourth section contains the simulation and experimental results to validate the proposed method and the last section has the discussion.

2. Multilevel Matrix Converter

2.1. Topology of MMC

A multilevel matrix converter (MMC) (Figure 1) consists of 18 bidirectional switches, $S_{Aa1} - S_{Cc2}$ and nine clamp capacitors, $C_1 - C_9$. The bidirectional switches constitute two integral semiconductor modules. The manufacturers, Yaskawa, ABB, Alstom, Siemens and so forth, have shown their interest in the production of these semiconductor power modules, consisting of bidirectional switches. In fact, Yaskawa has introduced many standard units of matrix converters of medium voltages and several megawatts.

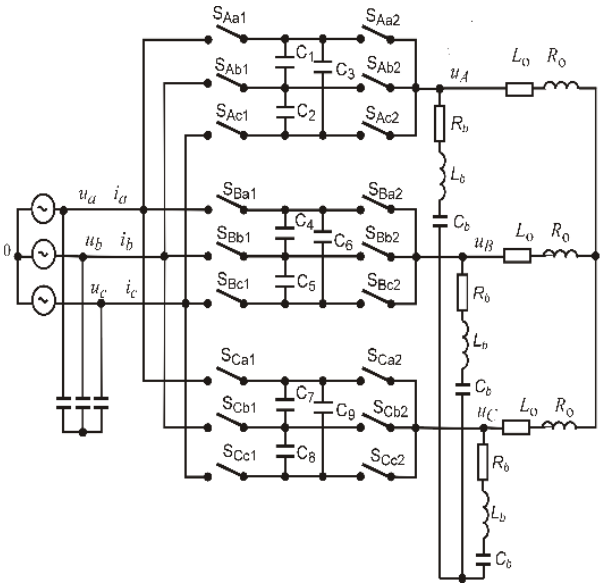

Figure 1. Scheme of multilevel matrix converter (MMC).

The clamp capacitors in MMC are connected by two switch matrixes and play a role analogous to flying capacitors in multicell converters, principally providing an additional intermediate voltage level in the process of synthesizing the output voltage. The capacitance of clamp capacitors depends on the value of the load current, switching the frequency and assumed value of the voltage ripple on the clamp capacitors [1–3]. Based on studies [1] and [24–26], concerned with the multicell converter, a capacitance value (1) of the capacitor should be determined using the admissible value of the voltage

ripple on that capacitor ΔU_C, number p of multilevel converter cells, load current I_o and switching frequency f_s of the converter switches.

$$C = \frac{I_o}{\Delta U_C p f_s} \tag{1}$$

To eliminate improper clamp capacitor voltages, shaping additional balancing circuits are used in MMC. The balancing circuit, providing an automatic maintenance of the clamp capacitor voltages, consists of R_b resistance, L_b inductance and C_b capacitance, connected in a series. The parameters of the balancing circuits are selected so that the resonance frequency f_o of those circuits is equal to the switching frequency f_s of the switches (2).

$$f_o = \frac{1}{2\pi\sqrt{L_b C_b}} = f_s \tag{2}$$

The resonance frequency is the most important parameter of the balancing circuit but the effectiveness of the balancing process, with a passive RLC circuit, depends also on the balancing circuit characteristic impedance, the converter parameters and the converter operating conditions [26,27].

2.2. Admissible Switch Configurations of MMC

Taking into account the voltage characteristics of the MMC supplying source, the switch configurations that do not make short circuit of the input phases and simultaneously assure the current path in the resistive-inductive load, are admissible. Therefore, each of the three output phases could be connected into one of the input phases directly through two series-connected bidirectional switches or through two switches and a clamp capacitor. Clamp capacitors C1 – C9 perform additional intermediate voltage levels in waveforms of the output voltage. In the ideal conditions of charging, voltages on the clamp capacitors should be equal to half of the appropriate line-line voltages (3).

$$\begin{aligned} u_{C1} = u_{C4} = u_{C7} &= (u_a - u_b)/2 \\ u_{C2} = u_{C5} = u_{C8} &= (u_b - u_c)/2 \\ u_{C3} = u_{C6} = u_{C9} &= (u_c - u_a)/2 \end{aligned} \tag{3}$$

As a result of the use of clamp capacitors, there exist additional current flow paths between the input and output phases. Taking into account only the admissible states of the bidirectional switches of MMC, each of the output phases may be connected with the three supply phases in nine different ways, corresponding to the converter configurations. These configurations arise from the 'on' or 'off' states of the bidirectional switches, which, for the output phase A, are shown in Table 1.

Table 1. Switch configuration of MMC in the output phase A.

	Switch State ('on': 1, 'off': 0)						**Instantaneous Value of Voltage in Output Phase A**
Configuration	S_{Aa1}	S_{Aa2}	S_{Ab1}	S_{Ab2}	S_{Ac1}	S_{Ac2}	
1	1	1	0	0	0	0	u_a
2	0	0	1	1	0	0	u_b
3	0	0	0	0	1	1	u_c
4	1	0	0	1	0	0	$(u_a+u_b)/2$
5	0	1	1	0	0	0	$(u_a+u_b)/2$
6	0	0	0	1	1	0	$(u_b + u_c)/2$
7	0	0	1	0	0	1	$(u_b + u_c)/2$
8	0	1	0	0	1	0	$(u_a + u_c)/2$
9	1	0	0	0	0	1	$(u_a + u_c)/2$

In the case of the first three configurations (1, 2, 3), shown in Table 1, every output phase is directly connected with one of the input phases, which is characteristic of a conventional MC. This means that the phase output voltage is equal the appropriate phase input voltage. The next six configurations (4, 5, 6, 7, 8, 9) implement the connections across clamp capacitors. For instance, while the switches S_{Aa1} and S_{Ab2} (configuration 4) or switches S_{Ab1} and S_{Aa2} (configuration 5) are 'on,' the current of the output phase A is running across the capacitor C_1 and connected in parallel capacitors C_2 and C_3. The instantaneous voltage of the output phase A is the same in both cases and equals $u_{C1} = (u_a + u_b)/2$, because of the voltage of the capacitor C_1 and because it is connected in parallel capacitors C_2 and C_3, equalling $(u_a - u_b)/2$. The choice between configurations 4 and 5 is the choice between different capacitor current directions, allowing for the possibility to control the capacitor voltage. The same regularity is fulfilled in the next two couples of configurations, that is, configurations 6 and 7 or 8 and 9. Recapitulating, we can conclude that each output phase can be connected to u_a, u_b, u_c, as the voltage supply (henceforth termed "full-amplitude voltage supply") or to $(u_a + u_b)/2$, $(u_b + u_c)/2$, $(u_a + u_c)/2$ (henceforth, "half-amplitude voltage supply").

Considering a three-phase to three-phase MMC, one has to take into account $9^3 = 729$ possible switch configurations, which can be used practically in the process of the synthesis of output voltages and the synthesis of the voltages of clamp capacitors, determining the intermediate levels of the supply voltages.

2.3. Output Voltage Space Vectors in MMC

The output voltages in three-input to three-output circuit of MMC could be presented using space vectors, as defined by (4). Instantaneous output voltages u_A, u_B and u_C in the relation (4) are appropriately equal to one of values defined in the output phase A in Table 1. The label xxx in the name $\vec{V}_{xxx}$ of the space vector means the type of configuration appropriately chosen in the output phase A, B and C.

$$\vec{V}_{xxx} = \frac{2}{3}\left[u_A + a u_B + a^2 u_C\right] \tag{4}$$

Analysis of the output voltages, corresponding to 729 switch configurations, allows for it to be noticed that the instantaneous output voltage space vectors could be split into the following groups:

- 27 zero space vectors, where the output voltages in each phase are the same;
- 360 active space vectors, where two of the output voltages have the same values; and
- 342 rotating space vectors.

The active voltage space vectors correspond to the connection of two output phases to the same voltage supply. The zero vectors arise when the output phases are connected with the same "full-amplitude voltage supply" or the same "half-amplitude voltage supply."

2.4. Output Voltage Space Vectors Reducing CMV in MMC

Among 342 configurations of MMC, with instantaneous output voltages represented by rotating space vectors, only 54 could be considered to reduce CMV. This conclusion is drawn from the analysis of rotating space vectors, determined with the assumption that the MMC is supplied by a balanced input voltage (5).

$$\begin{bmatrix} u_a \\ u_b \\ u_c \end{bmatrix} = \begin{bmatrix} U_{im}\cos\omega_i t \\ U_{im}\cos(\omega_i t - 120^\circ) \\ U_{im}\cos(\omega_i t + 120^\circ) \end{bmatrix} \tag{5}$$

All 342 rotating voltage space vectors representing instantaneous output voltages could be split into the following five groups:

- Rotating voltage space vectors, with a constant module equal to the amplitude of the input voltage U_{im}. These vectors correspond to switch configurations, where three output voltages are synthesized by the use of three full-amplitude supplying voltages. Six vectors belonging to this group create two sets, consisting of three rotating space vectors shifted by 120°. One set rotates in a positive direction (CCW vectors) along a complex plane and the next set rotates in a negative one (CW vectors). Two of these vectors are represented by Equations (6) and (7), as well as the relation (6)—for CCW vectors and (7)—for CW vectors. The digits in the label of the voltage vector name should be interpreted as follows: the first digit defines the configuration of the switches in the output phase A, the second and third digits, the output phase B and C, appropriately. The application of the rotating space vectors belonging to this group in the modulation of switch duty cycles results in a zero value of CMV (8).

$$\vec{V}_{123} = \frac{2}{3}\left[u_a + au_b + a^2u_c\right] = U_{im}e^{j\omega_i t} \tag{6}$$

$$\vec{V}_{132} = \frac{2}{3}\left[u_a + au_c + a^2u_b\right] = U_{im}e^{-j\omega_i t} \tag{7}$$

where: $a = e^{j120^\circ}$, $\quad a^2 = e^{j240^\circ}$

$$u_{CMV(123)} = \frac{u_a + u_b + u_c}{3} = 0 \tag{8}$$

- Rotating voltage space vectors, with a constant module equal to half of the input phase voltage amplitude that corresponds to 48 configurations with a connection of three output phases to three different half-amplitude voltage supplies. Half of these vectors complete 8 sets of three vectors rotating in a positive direction (CCW vectors) and half of them form 8 sets of vectors rotating in a negative one (CW vectors). Two of these vectors are assigned as (9) (CCW vectors) and (10) (CW vectors). The application of the rotating space vectors belonging to this group in the modulation of switch duty cycles also results in a zero value of CMV (11).

$$\vec{V}_{468} = \frac{2}{3}\left[\frac{1}{2}(u_a + u_b) + a\frac{1}{2}(u_b + u_c) + a^2\frac{1}{2}(u_a + u_c)\right] = -\frac{1}{2}U_{im}e^{j(\omega_i t - 120^\circ)} \tag{9}$$

$$\vec{V}_{486} = \frac{2}{3}\left[\frac{1}{2}(u_a + u_b) + a\frac{1}{2}(u_a + u_c) + a^2\frac{1}{2}(u_b + u_c)\right] = -\frac{1}{2}U_{im}e^{-j(\omega_i t + 120^\circ)} \tag{10}$$

$$u_{CMV(468)} = \frac{\frac{1}{2}(u_a + u_b) + \frac{1}{2}(u_b + u_c) + \frac{1}{2}(u_a + u_c)}{3} = 0 \tag{11}$$

- Rotating voltage space vectors, with a constant module equal to half of the input phase voltage amplitude, which corresponds to 72 configurations, with a connection of two output phases to two different half-amplitude voltage supplies and a third output phase connected to the full-amplitude voltage supply. Two examples are shown: CCW vector, as Equation (12) and CW vector, as Equation (13). The application in the modulation of switch duty cycles the rotating space vectors, belonging to the group being discussed, results in a value of CMV (14) that is not zero.

$$\vec{V}_{148} = \frac{2}{3}\left[u_a + a\frac{1}{2}(u_a + u_b) + a^2\frac{1}{2}(u_a + u_c)\right] = \frac{1}{2}U_{im}e^{j\omega_i t} \tag{12}$$

$$\vec{V}_{184} = \frac{2}{3}\left[u_a + a\frac{1}{2}(u_a + u_c) + a^2\frac{1}{2}(u_a + u_b)\right] = \frac{1}{2}U_{im}e^{-j\omega_i t} \tag{13}$$

$$u_{CMV(148)} = \frac{u_a + \frac{1}{2}(u_a + u_b) + \frac{1}{2}(u_a + u_c)}{3} = \frac{1}{2}u_a \tag{14}$$

- Rotating voltage space vectors, with a changeable module, that correspond to 72 configurations, with a connection of two output phases to two different full-amplitude voltage supplies and a third output phase connected to a half-amplitude voltage supply. The Equation (15) is an example of the vectors belonging to this group. The application of the rotating space vectors, belonging to this group, in the modulation of switch duty cycles, results in a value of CMV (16) that is not zero.

$$\begin{aligned}\vec{V}_{126} &= \tfrac{2}{3}\left[u_a + a u_b + a^2 \tfrac{1}{2}(u_b + u_c)\right] = U_{im} e^{j\omega_i t} + \tfrac{1}{3} a^2 u_{bc} \\ &= U_{im} e^{j\omega_i t} + \tfrac{\sqrt{3}}{3} U_{im} \sin \omega_i t \, e^{j240^\circ}\end{aligned} \tag{15}$$

$$u_{CMV(126)} = \frac{u_a + u_b + \frac{1}{2}(u_b + u_c)}{3} = \frac{1}{6} u_{bc} \tag{16}$$

- Rotating voltage space vectors, with a changeable module, that correspond to 144 configurations, with a connection of two output phases to two different half-amplitude voltage supplies and a third output phase connected to a full-amplitude voltage supply. The Equation (17) is an example of the vectors belonging to this group. The application of the rotating space vectors, belonging to this group, in the modulation of switch duty cycles, results in a value of CMV (18) that is not zero.

$$\begin{aligned}\vec{V}_{146} &= \frac{2}{3}\left[u_a + a\frac{1}{2}(u_a + u_b) + a^2 \frac{1}{2}(u_b + u_c)\right] = \\ &= U_{im} e^{j\omega_i t} - \frac{\sqrt{3}}{3} U_{im} \sin(\omega_i t - 60^\circ)\, e^{j120^\circ} + \frac{\sqrt{3}}{3} \sin\omega_i t \, e^{j240^\circ}\end{aligned} \tag{17}$$

$$u_{CMV(146)} = \frac{u_a + \frac{1}{2}(u_a + u_b) + \frac{1}{2}(u_b + u_c)}{3} = \frac{1}{6} u_{ac} \tag{18}$$

Finally, only 54 of the 729 switch configurations of MMC could be chosen, while the CMV elimination is required in the proposed control method. The lay-out of a complex plane of the rotating space vectors, belonging to the mentioned groups, is shown in Figure 2. In Figure 2, the initial position of the rotating space vectors is shown. The digits used in the label of vectors, instead of the full names of vectors, are shown in the figure.

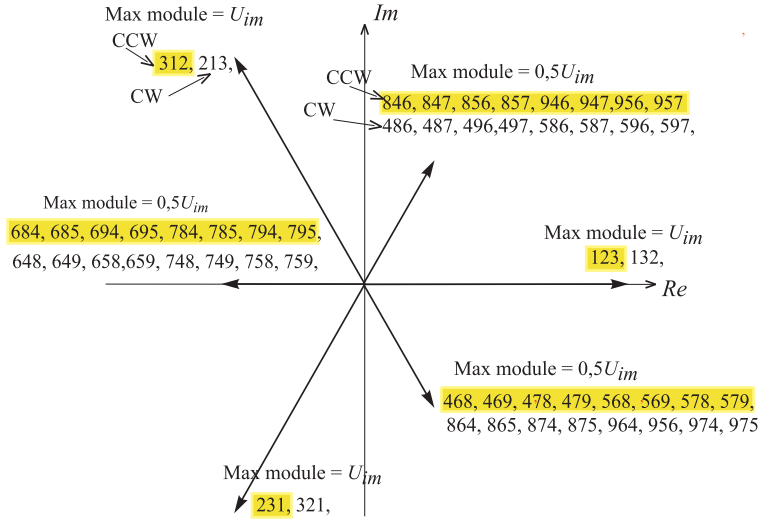

Figure 2. Lay-out of a complex plane of the voltage rotating space vectors, whose implementation assures the elimination of CMV.

The performed analysis of all of the allowable configuration of MMC and the corresponding voltage space vectors allows the vectors synthesizing the sinusoidal output voltage, sinusoidal input

current and elimination of CMV to be chosen. As a result, the proposed modulation method is based on the application solely of the switch configurations that correspond to the rotating space vectors, with a constant module. The rotating space vectors are not usually used in modulation strategies, because they lay in different positions, so it is difficult to create a repetitive pattern. However, in Reference [13], one can find that the implementation of the Venturini modulation function in the determination of switch duty cycles in conventional MC could provide the control using only rotating space vectors, while simultaneously eliminating CMV. By analogy, the Venturini modulation functions are used in the proposed strategy for modulation duty cycles in MMC.

3. Proposed modulation method

Method of the Output Voltage Synthesis

The synthesis of the output voltage by the use of rotating space vectors could be realized by applying a carrier-based implementation of SVM. The Venturini modulation functions are used in the proposed method to set out the switch duty cycles. The determination of the duty cycles for bidirectional switches of conventional MC and MMC by the use of Venturini modulation functions has been presented in References [13] and [2,3]. Here, the Venturini modulation function, in consideration of angle ψ, in the form of (19) or (20), is used. A value of angle ψ defines the phase shift between that defined by (5) input phase voltages and the appropriate output phase voltages. The application of the modulation function (19) results in CCW output voltage rotating space vectors and a lagging input displacement angle, whereas the modulation function (20) gives CW output voltage rotating space vectors and leading input displacement angle [2]. Both of them, that is, the modulation function (19), depending on the difference $\omega_o - \omega_i$ of the output and input frequency and modulation function (20), depending on the sum $\omega_o + \omega_i$ result in the output voltage amplitude, equal to half of the input voltage amplitude, at most.

$$\begin{array}{l} d_1^- = m_{Aa}^- = m_{Bb}^- = m_{Cc}^- = \frac{1}{3}\left(1 + 2k_U \cos(\omega_o - \omega_i)\, t + \psi\right) \\ d_2^- = m_{Ab}^- = m_{Bc}^- = m_{Ca}^- = \frac{1}{3}\left(1 + 2k_U \cos\left((\omega_o - \omega_i)\, t - \frac{2\pi}{3} + \psi\right)\right) \\ d_3^- = m_{Ac}^- = m_{Ba}^- = m_{Cb}^- = \frac{1}{3}\left(1 + 2k_U \cos\left((\omega_o - \omega_i)\, t + \frac{2\pi}{3} + \psi\right)\right) \end{array} \quad (19)$$

$$\begin{array}{l} d_1^+ = m_{Aa}^+ = m_{Bc}^+ = m_{Cb}^+ = \frac{1}{3}\left(1 + 2k_U \cos(\omega_o + \omega_i)\, t + \psi\right) \\ d_2^+ = m_{Ab}^+ = m_{Ba}^+ = m_{Cc}^+ = \frac{1}{3}\left(1 + 2k_U \cos\left((\omega_o + \omega_i)\, t - \frac{2\pi}{3} + \psi\right)\right) \\ d_3^+ = m_{Ac}^+ = m_{Bb}^+ = m_{Ca}^+ = \frac{1}{3}\left(1 + 2k_U \cos\left((\omega_o + \omega_i)\, t + \frac{2\pi}{3} + \psi\right)\right) \end{array} \quad (20)$$

As carrier signals, two-phase shifted carrier signals are adopted. The displacement of carrier signals, involved in the control of switches S_{ij1} and switches S_{ij2}, is $T_s/2$, where T_s is the carrier signal period. Duty cycles, in which switches S_{ij1} are switched-on, arise from the comparison of the corresponding modulation functions with one of the carrier signals. A carrier signal shifted by half of the switching cycle T_s determines the duty cycles of S_{ij2} switches (Figure 3). The digits in Figure 3, placed below the duty cycles, mean the numbers of configurations defined in Table 1. At the bottom in Figure 3, the names of the appropriate space vectors synthesizing the load voltage are placed. The mentioned vectors are the same as the rotating space vectors shown in Figure 2.

The application of modulation functions, with phase shift angle ψ, provides the phase shift between the output and the appropriate input voltage. This feature is important when the MMC works with the same input and output frequency and it allows the MMC to be used as a converter in Flexible AC Transmission System (FACTS) devices.

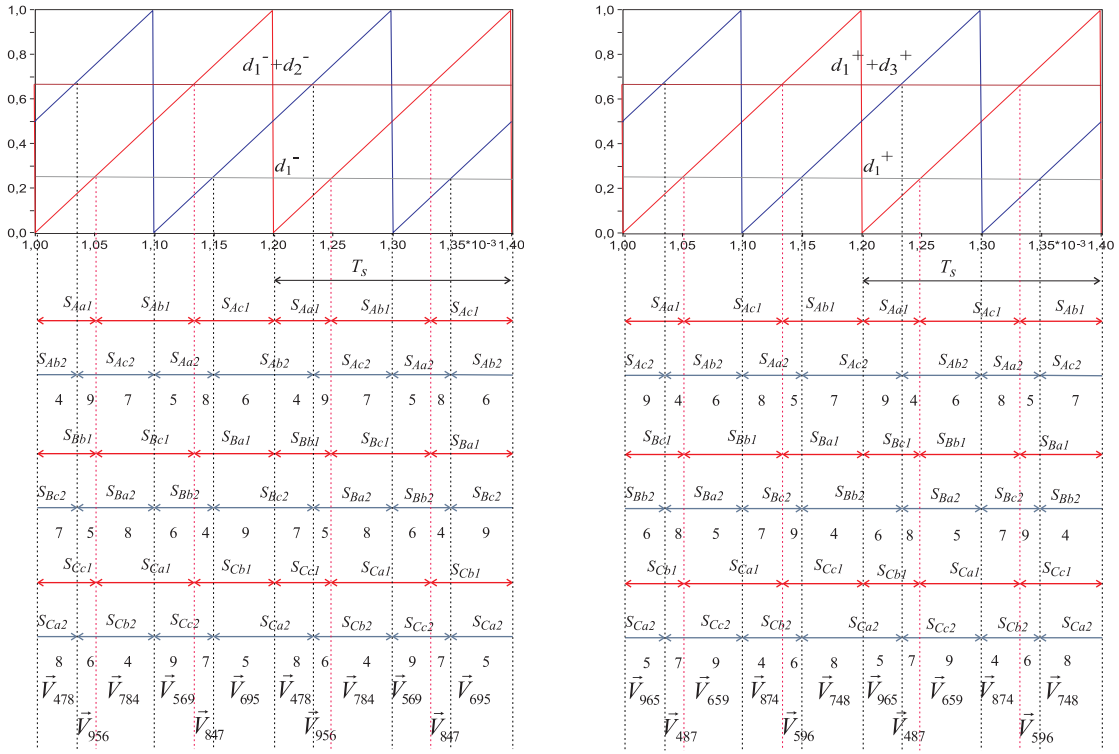

Figure 3. Switch duty cycles and rotating space vectors of the output voltage in MMC for CCW-type space vectors (**a**) and CW-type space vectors (**b**).

4. Simulation and Experiment

4.1. Simulation

Simulation tests were realized in an EMTP-ATP program. The matrix of the bidirectional switches was modelled as a matrix of the ideal bidirectional switches, controlled using signals generated in TACS subroutine. The supply grid is represented by ideal sinusoidal voltage sources, with an RMS value of 220 V and a frequency of 50 Hz, while the load consists in star-connected resistance and inductance elements, with values of 2 Ω and 10 mH. The carrier frequency was f_{carr} = 5 kHz. The capacitance of the clamp capacitors is equal 10μF. The performances obtained for MMC, controlled by the use of the carrier-based implementation of SVM combined with the Venturini modulation functions, are presented in Figures 4–7. The waveforms of the output voltage and CMV, as depicted in Figure 4 and in Figure 5, illustrate the control, with a lagging input displacement angle (CCW rotating space vectors). Waveforms in Figures 6 and 7 correspond to the leading input displacement angle, when the CW rotating space vectors are used. One can see that in both cases, the CMV is equal to zero. All these waveforms illustrate the control, with a value of the shift angle of $\psi = 0$. The Fourier analysis was performed, with an accuracy of 10 Hz. It could be observed that, besides fundamental harmonics, the output voltage consists of high frequency components, concentrated as sidebands around each multiple of the carrier frequency. However, it is also seen that, in comparison with conventional MC (Figure 8b), the amplitudes of the first group of these harmonics are significantly decreased. The comparison of the distortion components of the first groups in MC and MMC output voltages (Figures 4b and 8b), obtained with the same controlling parameters, indicates that the amplitude of these components decreased from 180.9 V in MC to 8.7 V in MMC. The waveforms chosen for presentation and FFT analysis prove that the applied modulation method results in a significant reduction of the distortion components of the MMC output voltage, compared with the MC output

voltage, which is a basic demand of a proper controlling method used for MMC. The second important feature of the proposed modulation method is the entire cancelation of CMV.

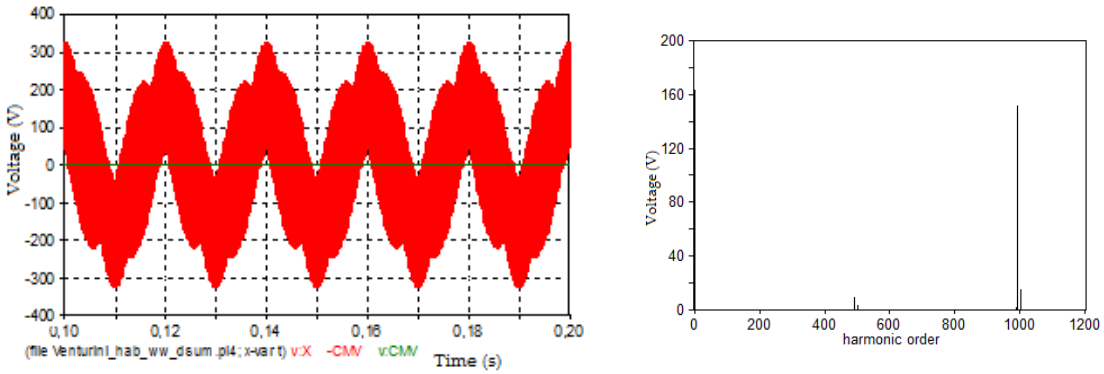

(**a**) (**b**)

Figure 4. Waveforms of the output voltages (red lines) and CMV (green lines) (**a**) and Fourier analysis of the output voltage (**b**), synthesized in MMC and controlled by the use of CCW rotating space vectors, for the angle $\psi = 0^\circ$ and output frequency of 50 Hz.

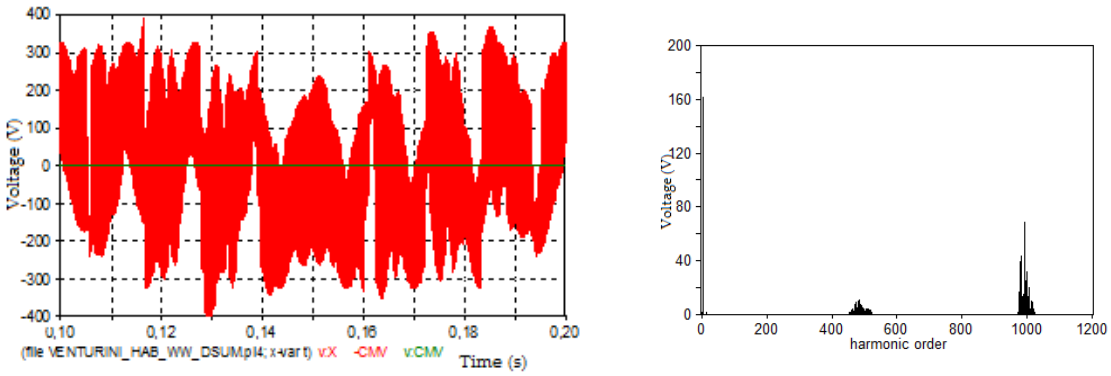

(**a**) (**b**)

Figure 5. Waveforms of the output voltages (red lines) and CMV (green lines) (**a**) and Fourier analysis of the output voltage (**b**), synthesized in MMC and controlled by the use of CCW rotating space vectors, for the angle $\psi = 0^\circ$ and output frequency of 80 Hz.

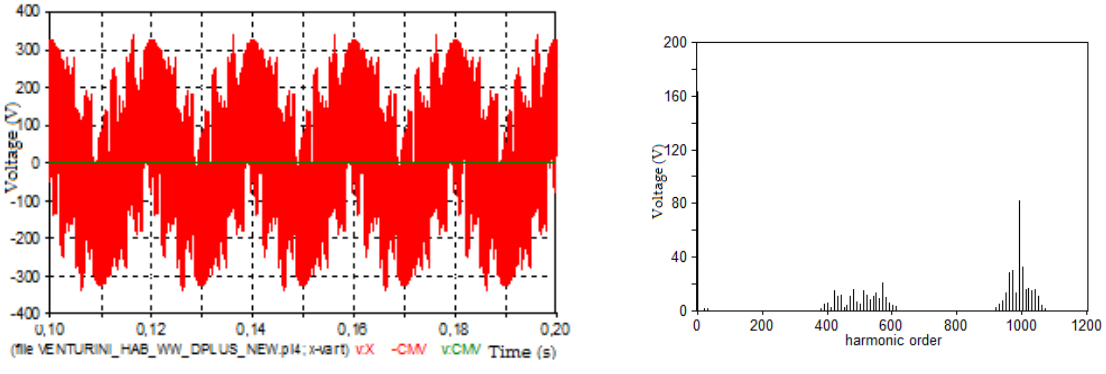

(**a**) (**b**)

Figure 6. Waveforms of the output voltages (red lines) and CMV (green line) (**a**) and Fourier analysis of the output voltage (**b**), synthesized in MMC and controlled by the use of CW rotating space vectors, for the angle $\psi = 0^\circ$ and output frequency of 50 Hz.

The next analysis (Figures 9 and 10) deals with the control of the phase shift between the output and input phase voltages. MMC works with the output frequency the same as it does with an

input one. In Figure 9, the waveform of the output voltages, together with the appropriate input voltages, for different shift angle values ψ between the input and output voltages, is shown. Performed simulation analysis proves that the control of the phase shift between the output and input voltage in MMC, controlled by the use of the carrier-based implementation of SVM, with Venturini modulation functions, is possible and is characterized by a linear relation (Figure 10).

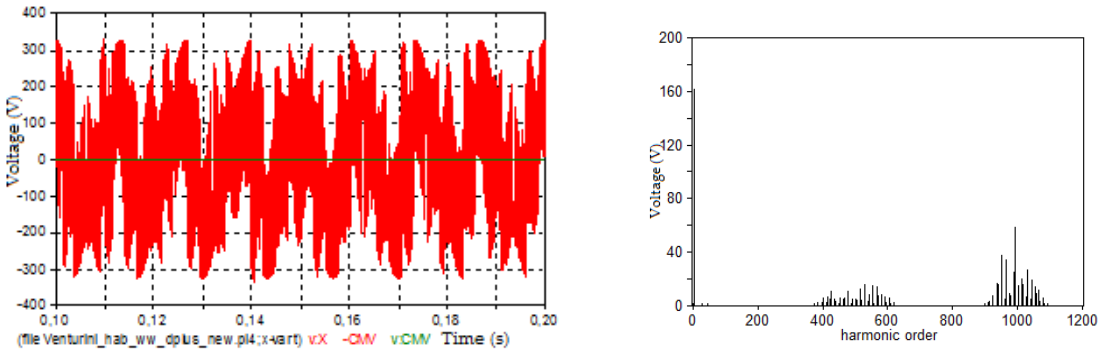

(**a**) (**b**)

Figure 7. Waveforms of the output voltages (red lines) and CMV (green line) (**a**) and Fourier analysis of the output voltage (**b**), synthesized in MMC and controlled by the use of CW rotating space vectors, for the angle $\psi = 0°$ and output frequency of 80 Hz.

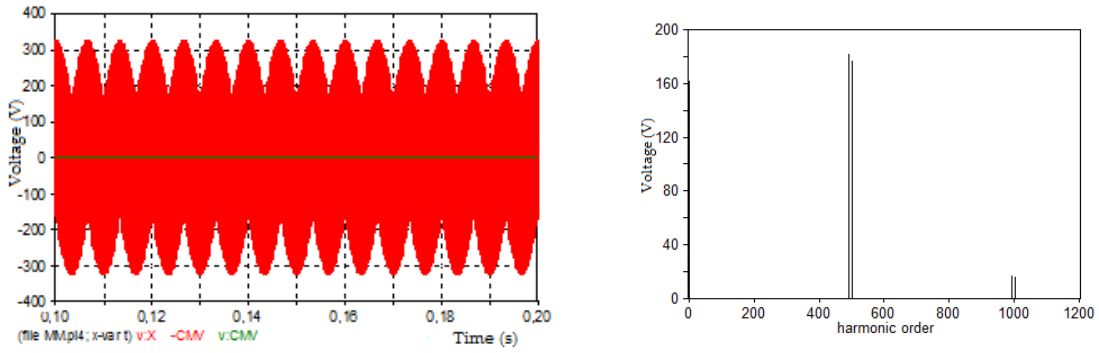

(**a**) (**b**)

Figure 8. Waveforms of the output voltage (red lines) and CMV (green line) (**a**) and Fourier analysis (**b**) of the output voltage, synthesized in conventional MC by the use of CCW rotating space vectors, for the output frequency of 50 Hz.

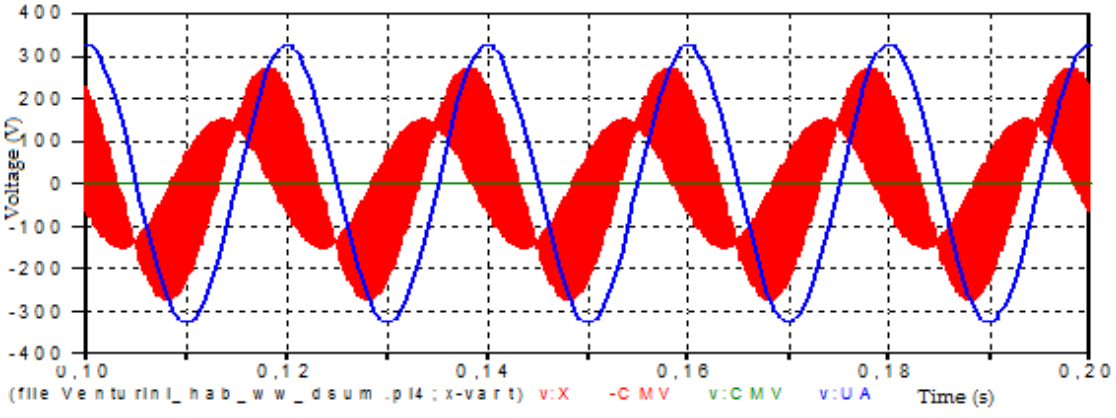

(**a**)

Figure 9. *Cont.*

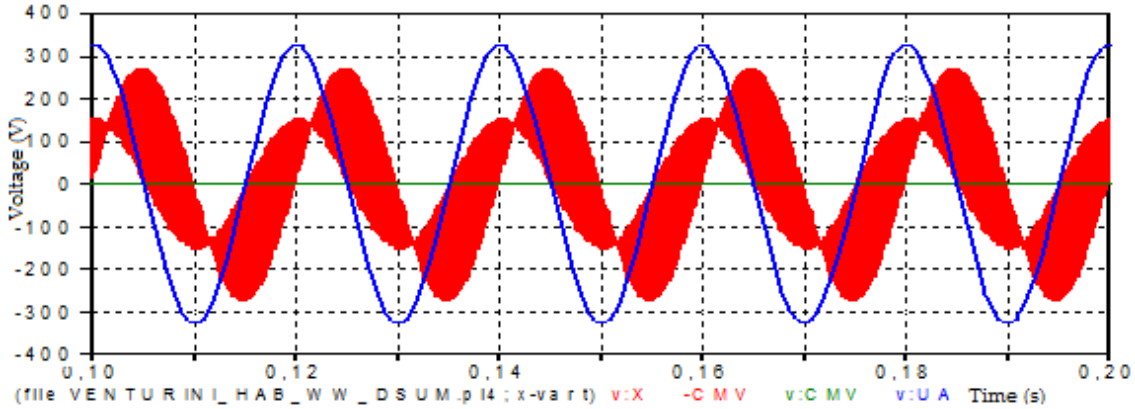

(**b**)

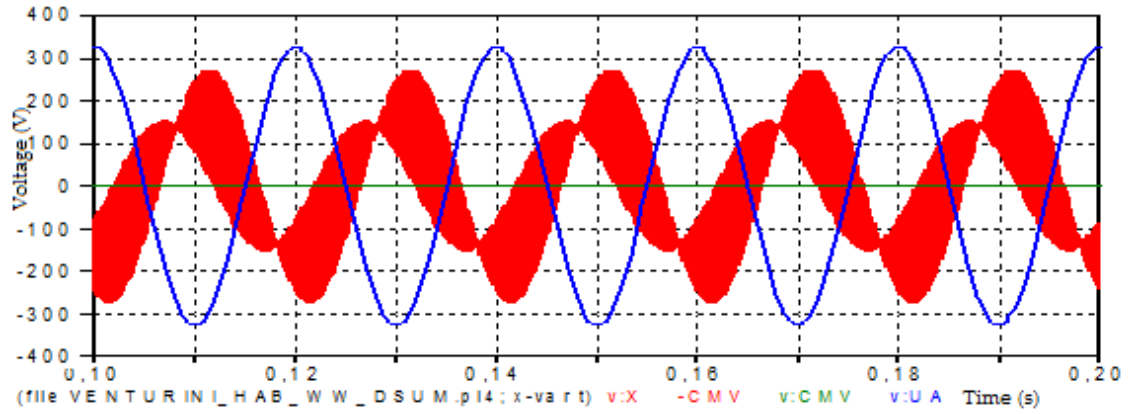

(**c**)

Figure 9. Waveform of the output voltages (red lines), input voltages (blue line) and CMV (green line) in MMC, controlled by the use of CCW rotating space vectors, for the output frequency of 50 Hz and angle $\psi = 60^\circ$ (**a**); angle $\psi = 6-0^\circ$ (**b**) and angle $\psi = 180^\circ$ (**c**).

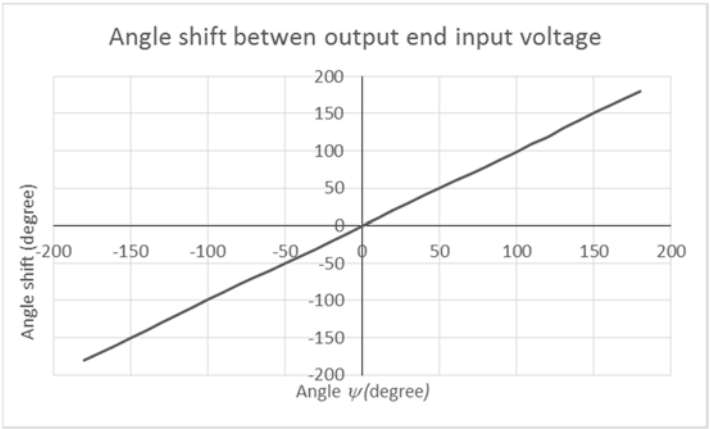

Figure 10. Angle shift between the output and input voltage versus the reference angle ψ.

4.2. Experiment

To further verify the proposed control method, measurement tests were performed. The experimental parameters are shown in Table 2.

Table 2. Experimental Parameters.

Parameter Name	Parameter Value
clamp capacitors C_1–C_9	1.1 µF
balancing circuit C_b; L_b; R_b	1 µF; 2.6 mH; 65 Ω
input frequency f	50 Hz
RMS value of input phase voltage	220 V
carrier frequency	5 kHz

Presented in Figures 11–13, waveforms represent the chosen results of measurements. They were registered in MMC, controlled by the use of modulation function (19) and were therefore the CCW-type rotating voltage space vectors. In Figure 11, the output voltage, together with the appropriate input voltage, is shown. The referenced angle shift is equal to 60°, −60° or 180° and the measurements confirm the accomplishment of these values. In Figure 12, the synthesized output voltage and CMV are shown. The maximum instantaneous values of CMV appear when the angle shift ψ is equal to −60° (Figure 12b). These maximum values of CMV do not exceed 40 V (Figure 13b), which is less than 12% of the peak values of the output voltage and amplitude of the input voltage.

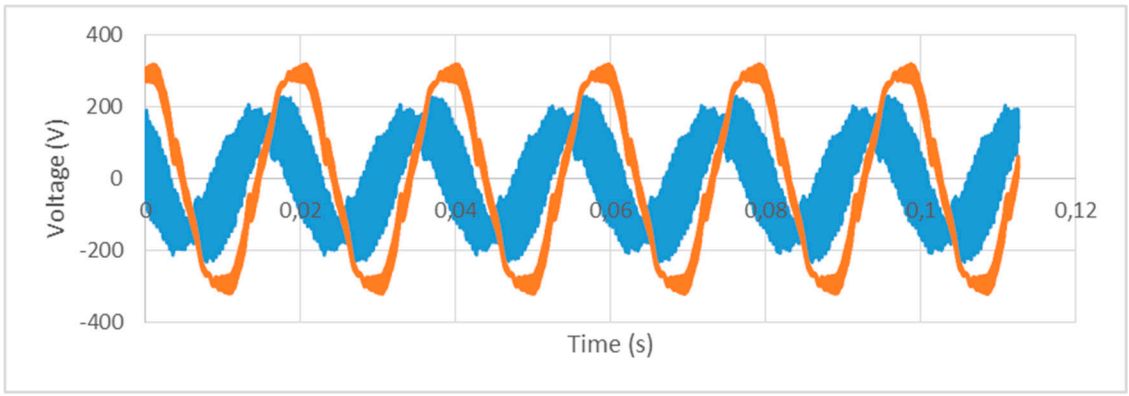

(a)

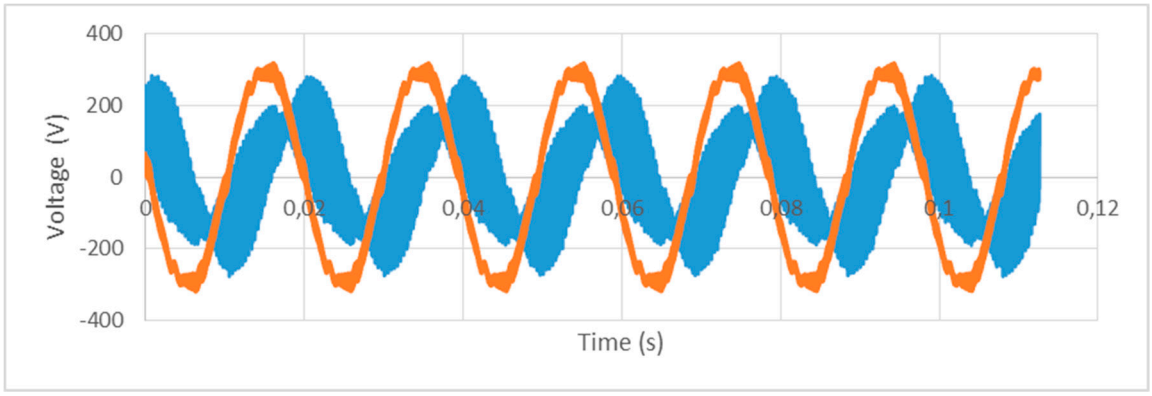

(b)

Figure 11. *Cont.*

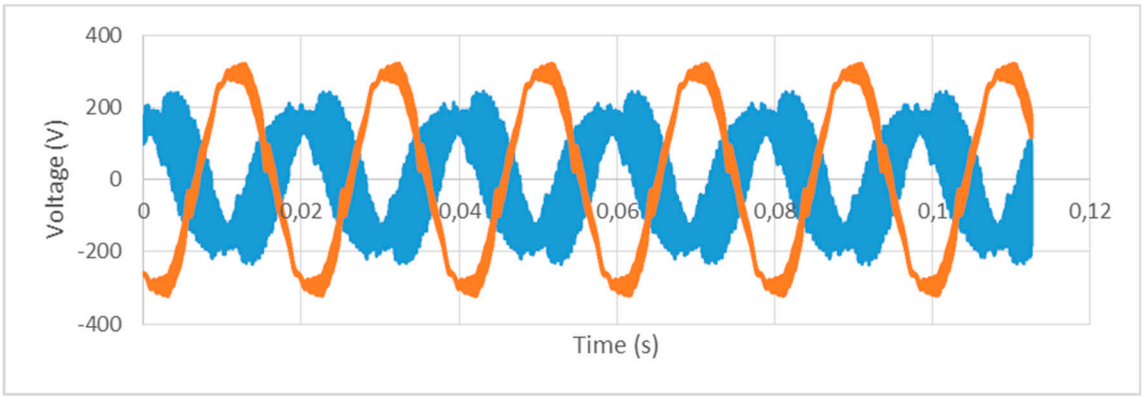

(c)

Figure 11. Waveform of the input phase voltage (orange) and output phase voltage (blue) for the referenced shift angle $\psi = 60°$ (**a**); $\psi = 6-0°$ (**b**) and $\psi = 180°$ (**c**).

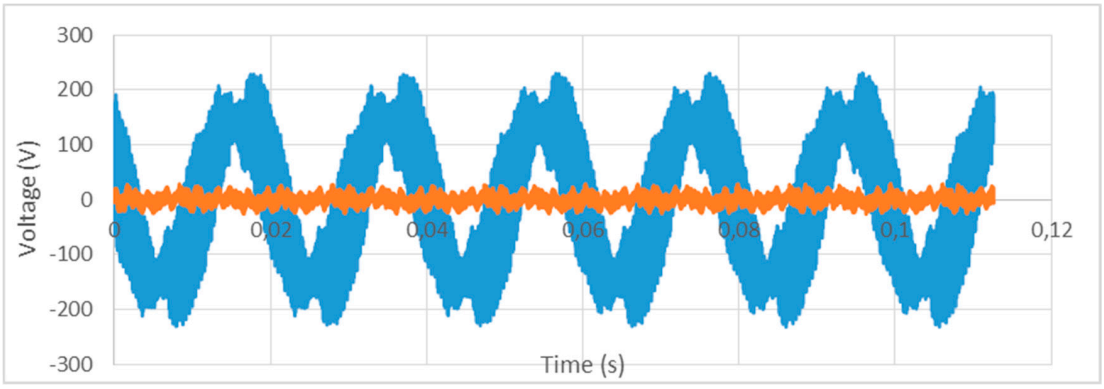

(a)

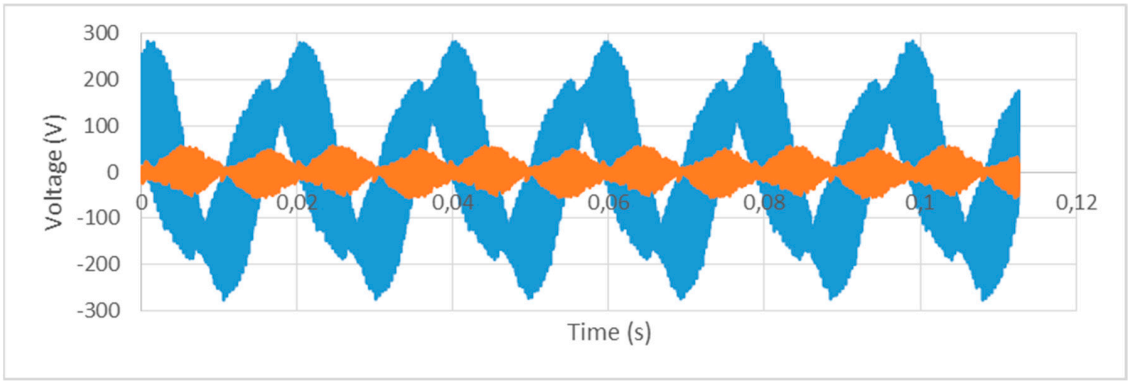

(b)

Figure 12. *Cont.*

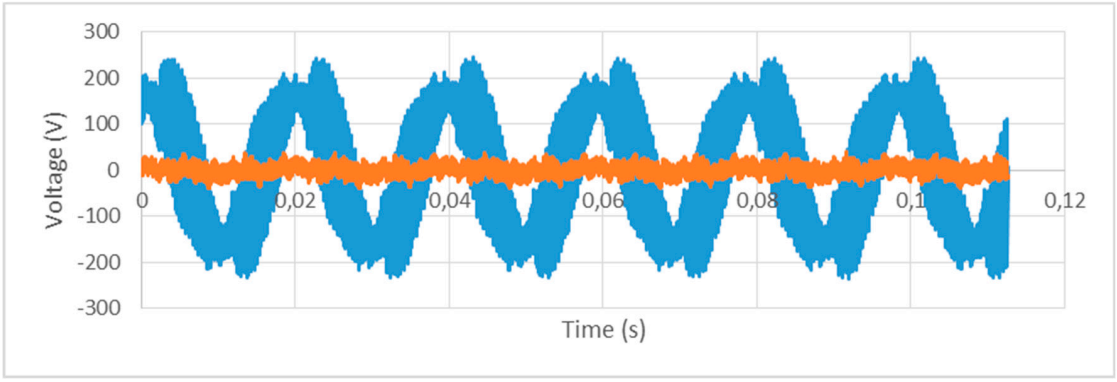

(c)

Figure 12. Waveform of the output phase voltage (blue) and CMV (orange), for the shift angle $\psi = 60°$ (**a**); $\psi = 6-0°$ (**b**) and $\psi = 180°$ (**c**).

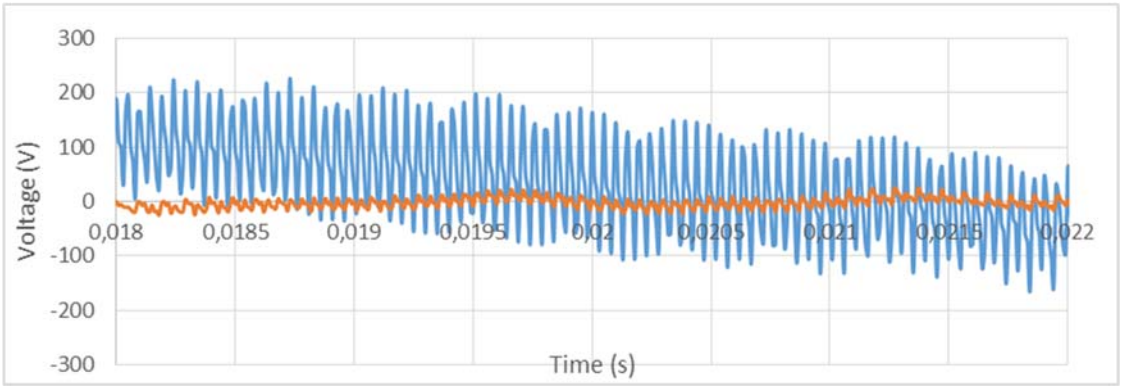

(**a**)

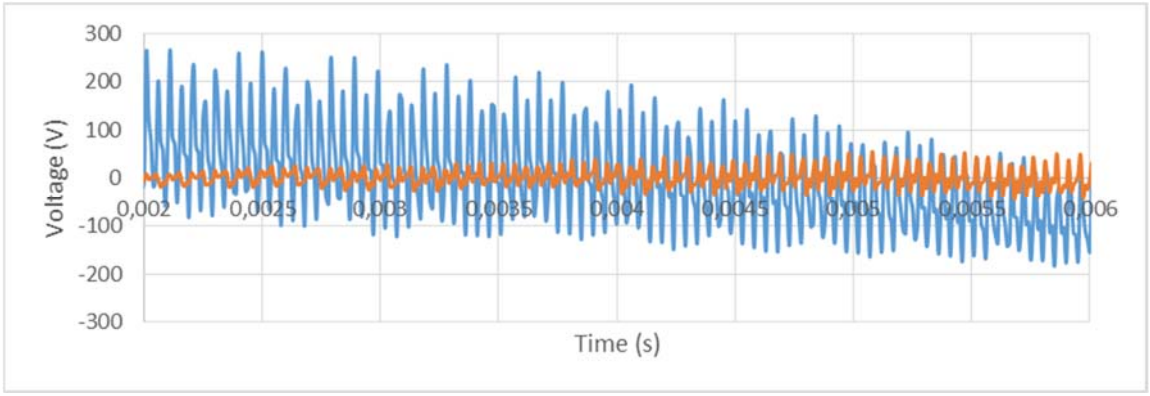

(**b**)

Figure 13. *Cont.*

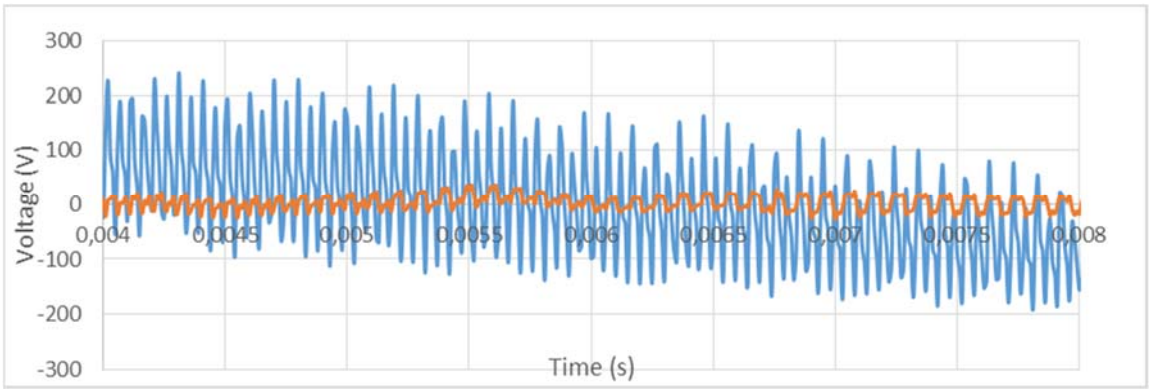

(**c**)

Figure 13. The enlarged waveform of the output phase voltage (blue) and CMV (orange), for the shift angle $\psi = 60^\circ$ (**a**); $\psi = 6-0^\circ$ (**b**) and $\psi = 180^\circ$ (**c**).

5. Discussion

The proposed carrier-based SVM, using Venturini modulation functions, is valuable because it realizes control whilst improving the waveform of the MMC output voltage compared with the MC output voltage. In MMC, controlled using the proposed method, the amplitudes of the first group of output voltage distortion components, concentrated near the first multiple of the carrier frequency, are only near 5% of the appropriate amplitude of output voltage distortion components in MC.

An important achievement, obtained by implementing the proposed modulation method, is the entire elimination of CMV, which was confirmed by the results of simulation tests. In the experiment, the peak value of CMV is less than 12% of the amplitude of the supplying voltage and the peak value of the output voltage. The occurrence of the CMV, measured higher than zero, may be explained by the noise activated by the four-step commutation process of the bidirectional switches. During the short period of the commutation steps, the active space vectors can appear and cause a higher than zero CMV. To avoid the problem with commutation noise, the four-step commutation in the experimental model of MMC should be modified in future research.

An additional advantage of the presented modulation method, not presented until now in the papers concerned with analysis of MMC, is the possibility to control the phase shift between the output voltage and the appropriate input voltage.

The drawback of the proposed controlling method is the fact that, using only rotating space vectors, the elimination of CMV is possible; this is concerned with the application of modulation functions, which determine the constant input displacement angle between the input voltage and the phase current. On the other hand, this feature may be utilized in FACTS devices that realize series compensation when the input terminals of MMC are connected with the supply network in a shunt manner. MMC, controlled using CW rotating space vectors (modulation function (20)) at the input terminals, draws the current which precedes the appropriate supplying voltage, so MMC works as a source of reactive power for the AC system and also realizes shunt compensation.

Funding: This research received no external funding.

Conflicts of Interest: The author declares no conflict of interest.

Abbreviations

AC	Alternating Current
CCW rotating space vector	Counter Clockwise rotating space vector
CMV	Common mode Voltage
CW	Clockwise rotating space vector
DC	Direct Current
EMTP-ATP	Electromagnetic Transients Program—with version ATP
FACTS	Flexible AC Transmission System
FFT	Fast Fourier Transformation
MC	Matrix Converter
MMC	Multilevel Matrix Converter
PWM	Pulse Width Modulation
SVM	Space Vector Modulation
VTR	Voltage Transfer Ratio

References

1. Shi, Y.; Yang, X.; He, Q.; Wang, Z. Research on Novel Capacitor Clamped Multilevel Matrix Converter. *IEEE Trans. Power Electron.* **2005**, *20*, 1055–1065. [CrossRef]
2. Rząsa, J. Multilevel Matrix Converter Controlled with use of Venturini Method. *Przegląd Elektrotechniczny Rok* **2007**, *Nr 2*, 57–64. (In Polish)
3. Rząsa, J. Capacitor Clamped Multilevel Matrix Converter Controlled with Venturini Method. In Proceedings of the EPE-PEMC, Poznań, Poland, 1–3 September 2008.
4. Rząsa, J. Switch Current Harmonic Distortion in Classic and Capacitor-Clamped Multilevel Matrix Converters. In Proceedings of the 35th Annual Conference of the IEEE Industrial Electronics Society IECON'09, Porto, Portugal, 3–5 November 2009.
5. Lie, X.; Clare, J.C.; Wheeler, P.W.; Empringham, L. Space Vector Modulation for a Capacitor Clamped Multi-level Matrix Converter. In Proceedings of the EPE-PEMC 2008 13th International Power Electronics and Motion Conference, Poznań, Poland, 1–3 September 2008.
6. Lie, X.; Clare, J.C.; Wheeler, P.W.; Empringham, L. Capacitor Clamped Multi-Level Matrix Converter: Space Vector Modulation and Capacitor Balance. In Proceedings of the 2008 34th Annual Conference of IEEE Industrial Electronics, Orlando, FL, USA, 10–13 November 2008.
7. Lie, X.; Yongdong, L.; Kui, W.; Clare, J.C.; Wheeler, P.W. Research on the Amplitude Coefficient for Multilevel Matrix Converter Space Vector Modulation. *IEEE Trans. Power Electron.* **2012**, *27*, 3544–3556. [CrossRef]
8. Lie, X.; Clare, J.C.; Wheeler, P.W.; Empringham, L.; Yongdong, L. Capacitor Clamped Multilevel Matrix Converter Space Vector Modulation. *IEEE Trans. Ind. Electron.* **2012**, *59*, 105–115. [CrossRef]
9. Espina, J.; Ortega, C.; de Lillo, L.; Empringham, L.; Balcells, J.; Arias, A. Reduction of Output Common Mode Voltage Using a Novel SVM Implementation in Matrix Converters for Improved Motor Lifetime. *IEEE Trans. Ind. Electron.* **2014**, *61*, 5903–5911. [CrossRef]
10. Espina, J.; Arias, A.; Balcells, J.; Ortega, C. Common mode output waveforms reduction for Matrix Converters drives. In Proceedings of the 2009 35th Annual Conference of IEEE Industrial Electronics, Porto, Portugal, 3–5 November 2009; pp. 4499–4504. [CrossRef]
11. Guan, Q.; Wheeler, P.; Guan, Q.; Yang, P. Common-mode voltage reduction for matrix converters using all valid switch states. *IEEE Trans. Power Electron.* **2016**, *31*, 8247–8259. [CrossRef]
12. Padhee, V.; Sahoo, A.K.; Mohan, N. Modulation technique for common mode voltage reduction in a matrix converter drive operating with high voltage transfer ratio. In Proceedings of the 2016 IEEE Applied Power Electronics Conference and Exposition (APEC), Long Beach, CA, USA, 20–24 March 2016; pp. 1982–1988. [CrossRef]
13. Rzasa, J. Control of a matrix converter with reduction of a common mode voltage. In Proceedings of the IEEE Compatibility in Power Electronics, Gdynia, Poland, 6 January 2005.
14. Nguyen, H.; Lee, H. A Modulation Scheme for Matrix Converters with Perfect Zero Common-Mode Voltage. *IEEE Trans. Power Electron.* **2016**, *31*, 5411–5422. [CrossRef]

15. Mohapatra, K.K.; Ned, M. Open-End Winding Induction Motor Driven with Matrix Converter for Common-Mode Elimination. In Proceedings of the Power Electronics, Drives and Energy Systems, New Delhi, India, 12–15 December 2006.
16. Gupta, R.K.; Mohapatra, K.K.; Somani, A.; Mohan, N. Direct-Matrix-Converter-Based Drive for a Three-Phase Open-End-Winding AC Machine with Advanced Features. *IEEE Trans. Ind. Electron.* **2010**, *57*, 4032–4042. [CrossRef]
17. Tewari, S.; Mohan, N. Matrix Converter Based Open-End Winding Drives with Common-Mode Elimination: Topologies, Analysis, and Comparison. *IEEE Trans. Power Electron.* **2018**, *33*, 8578–8595. [CrossRef]
18. Rząsa, J. Research on Dual Matrix Cnverter Feeding an Open-End-Winding Load Controlled with the Use of Rotating Space Vectors. Part I. In Proceedings of the 39th Annual Conference of the IEEE Industrial Electronics Society IECON 2013, Vienna, Austria, 10–13 November 2013.
19. Rząsa, J.; Garus, G. Research on Dual Matrix Converter Feeding an Open-End-Winding Load Controlled with the Use of Rotating Space Vectors. Part II. In Proceedings of the 39th Annual Conference of the IEEE Industrial Electronics Society IECON 2013, Vienna, Austria, 10–13 November 2013.
20. Baranwal, R.; Basu, K.; Mohan, N. An alternative carrier based implementation of Space Vector PWM for dual matrix converter drive with common mode voltage elimination. In Proceedings of the IECON 2014—40th Annual Conference of the IEEE Industrial Electronics Society, Dallas, TX, USA, 29 October–1 November 2014; pp. 1208–1213. [CrossRef]
21. Jianglei, Q.; Lie, X.; Wang, L.; Lin, Q.; Yongdong, L. The modulation of common mode voltage suppression for a three-level matrix converter. In Proceedings of the 2016 IEEE International Conference on Aircraft Utility Systems (AUS), Beijing, China, 10–12 October 2016; pp. 533–538. [CrossRef]
22. Jianglei, Q.; Lie, X.; Lina, W.; Yannian, H. Research on the modulation and control of multilevel matrix converter. *J. Eng.* **2018**, *2018*, 614–621. [CrossRef]
23. Monteiro, J.; Silva, J.F.; Pinto, S.G.; Palma, J. Matrix Converter-Based Unified Power-Flow Controllers: Advanced Direct Power Control Method. *IEEE Trans. Power Deliv.* **2011**, *26*, 420–430. [CrossRef]
24. Meynard, H.; Foch, T.A.; Thomas, P.; Courault, J.; Jakob, R.; Nahrstaedt, M. Multicell Converters: Basic Concepts and Industry Applications. *IEEE Trans. Ind. Electron.* **2002**, *49*, 978–987. [CrossRef]
25. Meynard, T.A.; Fadel, M.; Aouda, N. Modeling of Multilevel Converters. *IEEE Trans. Power Electron.* **1997**, *44*, 356–364. [CrossRef]
26. Pirog, S.; Stala, R. Selection of parameters for a balancing circuit of dc–dc and ac–ac multicell converters. In Proceedings of the 2005 European Conference on Power Electronics and Applications, Dresden, Germany, 11–14 September 2005; p. 910.
27. Stala, R.; Mondzik, A. A study of the balancing process in multicell ac/ac converter. *Przegląd Elektrotechniczny* **2009**, *nr 7*, 168–172.